ELSEVIER

J. Non-Newtonian Fluid Mech. 94 (2000) 135–149

Journal of Non-Newtonian Fluid Mechanics

www.elsevier.com/locate/jnnfm

A unified wall slip model

Yogesh M. Joshi [a], Ashish K. Lele [a], R.A. Mashelkar [b,*]

[a] *Chemical Engineering Division, National Chemical Laboratory, Pune 411008, India*
[b] *Council of Scientific and Industrial Research, Anusandhan Bhavan, 2 Rafi Marg, New Delhi 110001, India*

Received 10 May 2000; received in revised form 10 July 2000

Abstract

A unified slip model is developed, which predicts wall slip by either a disentanglement mechanism or by debonding mechanism, depending upon the adhesive energy of the wall-polymer pair. The model is based on the transient network theory, in which the activation processes of adsorption and desorption are considered to occur at the wall in parallel to the stretching of the adsorbed chains. It is shown that the stick–slip transition occurs due to the local non-monotonic flow behavior near the wall irrespective of the mechanism of slip. The model predictions of the critical wall shear stress are in good agreement with experimentally observed values of the critical stress for various adhesive energies of wall polymer pair. Another important prediction of the model is that the temperature dependence of the critical wall shear stress for debonding is different than that of disentanglement mechanism under certain experimental conditions. This may be useful for discerning the correct mechanism of slip. The unified model encompasses different systems (viz. entangled solutions and melts) and diverse mechanisms (viz. disentanglement and debonding) in a common mathematical framework.

Keywords: Slip; Unified model; Transient network model; Disentanglement; Debonding; Temperature dependence

1. Introduction

Although the no-slip boundary condition at the fluid–solid interface has been a text book prescription for students of fluid mechanics, the occurrence of sudden slippage at the wall under certain conditions in structured fluids has been a challenging problem in fluid mechanics. Wall slip in polymer solutions and melts in particular has been a subject of intense investigation for the past several decades and has been recently reviewed by several authors [1,2]. Many mechanisms have been proposed to explain this phenomenon but those that have received wider acceptance in recent years are polymer chain disentanglement [3] and debonding [4] at the wall–polymer interface. Many models were developed earlier, which proposed that slip occurs by constitutive (bulk) instability [5–7]. However, it has now been shown

* Corresponding author. Fax: +91-11-971-0618.
E-mail address: dgcsir@csir.res.in (R.A. Mashelkar).

0377-0257/00/$ – see front matter
PII: S0377-0257(00)00160-9

unambiguously that slip is an interfacial phenomenon that occurs very close to the wall. [8]. Although the mechanisms for wall-slip are fairly well understood, there are several issues that still remain unresolved. For example, the dynamics of polymer chains at the wall is not yet well understood, and so is the effect of molecular parameters such as molecular weight distribution and long and short chain branching.

The physical manifestation of slip shows up in terms of experimental observations of the existence of a critical wall-shear stress, flow oscillations, extrudate distortion, hysteresis and temperature dependence of critical wall-shear stress. However, by merely observing a given manifestation in a given set of experimental data, it has not been possible so far to a priori assign a mechanism, be it debonding or disentanglement. Indeed the same experimental data on slip for the same polymer have been interpreted in terms of both disentanglement as well as debonding. For example, the experimental data on wall slip for common systems such as polyethylene in steel capillaries has been described by theoretical arguments of debonding [4] as well as disentanglement [9]. It is important to recognize that the physical basis and the mathematical frameworks for debonding and disentanglement are completely different. It is generally believed that the magnitude of the energy of adhesion between the wall and the adsorbed polymer chains will determine the governing mechanism of slip. We believe that a unified model, which can predict slip by both debonding and disentanglement mechanisms and which can distinguish between the two mechanisms on basis of the relative role of adhesive energy will be helpful in ascribing the correct mechanism to given experimental slip data. In this paper, we develop a unified slip model to address this issue.

The unified slip model in this work is based on the transient network (TN) formalism, which naturally considers the dynamics of chain entanglement and disentanglement under flow. Therefore, we will show that the model is naturally able to predict wall slip by an interfacial instability caused by a sudden disentanglement of the tethered chains from the bulk chains at a critical stress. Our unified model also considers the dynamics of adsorption and desorption of chains at the wall in parallel to the entanglement–disentanglement dynamics. Since the adsorption–desorption processes strongly depend on the adhesive energy between the polymer and the wall, the model predicts slip to occur by debonding of chains at the wall for low adhesive energies and by disentanglement of chains at the wall for high adhesive energies. Thus, unification of the two mechanisms of slip is achieved in a single mathematical framework.

Our approach as outlined distinctly differs from earlier slip models. Hill [4] developed a slip model by postulating only a debonding mechanism. Brochard and de Gennes [3], Adjari et al. [10] and Brochard-Wyart et al. [11] developed scaling models only by postulating disentanglement mechanisms. Hatzikiriakos and Kalogerakis [12] developed a slip model based on the TN formalism, but considered only the strain induced debonding of tethered segments above a critical strain. Thus, their model is specifically based on a debonding mechanism. Recently Yarin and Graham [13] have proposed a slip model based on the proposition that the lifetime of a tethered chain under shear flow is proportional to the excess energy gained by the tethered molecule due to flow. In the case, where the detachment of tethered chains precedes disentanglement, they predict that the shear stress–slip velocity relationship becomes non-monotonic due to the desorption of tethered chains. Thus, their model is essentially a debonding model. They also predict that when slip occurs by debonding, the slip length (see Eq. (16)) is independent of temperature so that the temperature independence of the slip length may not be an appropriate criterion for assigning the slip mechanism to be disentanglement driven. This is contrary to the hypothesis of Wang and Drda [14], who infer that the temperature invariance of the slip length along with the time–temperature superposition of slip data necessarily indicate slip by disentanglement. It is clear that none of the models developed so far have addressed the issue of the unification of the two mechanisms of slip in the same manner as the slip model described here.

The physical basis of the unified model has been partially developed in our previous work [15], in which the interfacial polymer layer between the wall and the bulk fluid was considered to be an annular region with a thickness of approximately one radius of gyration. It was argued that the dynamics of adsorbed interfacial molecules is different from that of the bulk molecules. We showed that the transient network model predicts disentanglement of the adsorbed molecules from the bulk chains at a critical wall-shear stress. The model also successfully predicted a first-order transition in the flow rate at the critical wall-shear stress. Further it predicted a direct proportionality between the temperature and the critical wall-shear stress, which is similar to the prediction made by Brochard and de Gennes [3]. Finally, the model also predicted the diameter dependence of the flow curves, hysteresis and the possibility of fluctuations in flow rate and pressure during extrusion. We showed that the model predicts wall slip in polymer melts as well as solutions, thus unifying different systems showing slip. However, the model considered slip solely by the disentanglement of adsorbed chains, completely disregarding debonding. Our previous work forms a natural platform on which we build a new model, which will unify the two mechanisms of slip, i.e. debonding and disentanglement, into one self-consistent framework.

Our model is semi-empirical in nature and contains adjustable parameters arising from the phenomenological nature of the rates of creation and breakage of network. While this approach does not throw light on the details of molecular dynamics of polymer chains near the wall, it has the inherent advantage of presenting a simpler constitutive equation that captures the essence of slip phenomena by either of the two physical mechanisms. Such a constitutive equation could be useful for providing numerical solutions to real engineering problems. Our model is the only one today which correctly predicts the temperature dependence of critical stress for slip and also shows that this dependence provides a useful tool for discerning the true mechanism of slip.

2. Theoretical

We begin by postulating the existence of the interfacial layer at the capillary wall, wherein the molecules are sparsely adsorbed on to the wall (the mushroom region) and their tails are entangled with the bulk. The interfacial layer can be considered to be a transient network made up of two types of network junctions (see Fig. 1): one consisting of the junctions on the wall, where the molecules are adsorbed, and the other consisting of the entanglement points with the bulk chains. The nature of these two types of network junctions is different in terms of their energetics and dynamics, as will be discussed later. We postulate that when both these types of junctions remain intact, no-slip boundary condition prevails. Slip occurs when any one of the types of junctions is destroyed. If the junctions at the wall are destroyed, then the slip occurs by debonding. When the entanglement junctions are destroyed, the slip occurs by disentanglement.

For simplicity, we assume that a polymer molecule adsorbs at a single site on the wall and has a Gaussian configuration. Let P_w be the number of chains per unit area adsorbed on the wall, P be the number of bulk polymer molecules per unit area coming into contact with the bare wall and w be the number of the bare sites per unit area on the wall on which a molecule can adsorb. Then the adsorption–desorption process can be represented in the framework of a reversible chemical reaction as

$$P_w \underset{k_a}{\overset{k_d}{\rightleftarrows}} P + w, \tag{1}$$

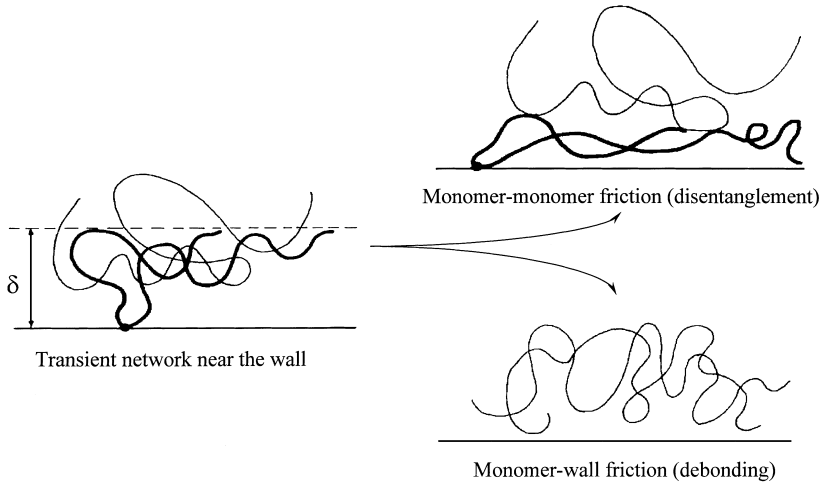

Fig. 1. A schematic of wall slip mechanisms. Slip due to both debonding and disentanglement mechanism can be seen.

where k_a and k_d are kinetic rate constants for adsorption and desorption reactions, respectively. From Eq. (1)

$$\frac{d[P_w]}{dt} = k_a[P][w] - k_d[P_w]. \tag{2}$$

Let w_t be the total number of sites per unit area on which a polymer molecule can adsorb, then

$$w_t = P_w + w. \tag{3}$$

Since the kinetics of adsorption and desorption are extremely fast as compared to the processes occurring on a rheological time scale [4], it is appropriate to assume that pseudo-equilibrium condition holds. Then from Eqs. (2) and (3) we get

$$\phi = \frac{[P_w]}{[w_t]} = \frac{k_a[P]}{k_a[P] + k_d}. \tag{4}$$

Here, ϕ is the fractional surface coverage. Since the concentration of the unattached polymer molecules near the wall is very high, it can be assumed to be approximately constant.

The kinetic coefficients in Eq. (4) can be defined as a product of the pre-exponential frequency factor and an activation term (similar to that used by Hill [4]).

$$k_a[P] = A\frac{kT}{h}\exp\left(\frac{-\Delta E_a}{kT}\right), \qquad k_d = \frac{kT}{h}\exp\left(\frac{-\Delta E_d + \Delta E_m}{kT}\right), \tag{5}$$

where ΔE_a is the activation energy for adsorption, ΔE_d is the activation energy for desorption, ΔE_m is the elastic free energy of the attached molecule relative to the equilibrium (no-flow) state, h is Plank's constant and A is a parameter that converts the second-order rate constant k_a into a pseudo-first-order rate constant. It is important to note that we have assumed the desorption rate to be proportional to the elastic (recoverable) energy of the adsorbed molecule.

The free energy of the attached molecule relative to the equilibrium (no-flow) state can be written as [16]

$$\Delta E_{\mathrm{m}} = \frac{3}{2}kT\frac{\langle R^2\rangle}{\langle R^2\rangle_0} - \Delta E_{\mathrm{eq}}, \tag{6}$$

$$\Delta E_{\mathrm{eq}} = \tfrac{3}{2}kT. \tag{7}$$

Here, subscript 0 represents unperturbed conditions (no flow). If it is assumed that the effective strain on the adsorbed molecule can be substituted by the effective elastic strain, then

$$\gamma_{\mathrm{e}}^2 \sim \left(\frac{\langle R^2\rangle}{\langle R^2\rangle_0} - 1\right), \tag{8}$$

where $\gamma_{\mathrm{e}} = (\tau_{zz} - \tau_{rr})/2\tau_{rz}$. For simplicity we assume that the constant of proportionality in Eq. (8) is unity. We feel that this is a reasonable assumption to make in the view of the fact that the network deforms affinely at low stress values. The approximation of substituting γ_{e} in place of the actual strain on a molecule allows one to derive a closed form constitutive relation for the shear stress as will be seen later. This approximation is further justified by the fact that the axial strain on molecules in laminar capillary flow is proportional to the normal stress [17], which is considered in γ_{e}. From Eqs. (5), (6) and (8), the kinetic rate constant for desorption can be written as

$$k_{\mathrm{d}} = \frac{k\mathrm{T}}{h}\exp\left(-\frac{\Delta E_{\mathrm{d}}}{kT} + \frac{3}{2}\gamma_{\mathrm{e}}^2\right). \tag{9}$$

The above form of the kinetic rate constant for desorption implicitly takes into account the effect of temperature. The desorption rate is proportional to the energy of the adsorbed molecule, which is directly proportional to the product of the tension in the molecule and the strain experienced by the adsorbed molecule. Note that at constant wall-shear stress, the tension in the adsorbed molecule remains independent of temperature but the strain in the molecule decreases with an increase in temperature due to increased stiffness.

Insertion of Eqs. (5) and (9) into Eq. (4) gives the final expression for surface coverage

$$\phi = \frac{A\exp([\Delta E_{\mathrm{adh}}]/kT)}{A\exp([\Delta E_{\mathrm{adh}}]/kT) + \exp((3/2)\gamma_{\mathrm{e}}^2)}, \tag{10}$$

where ΔE_{adh} is the adhesive energy ($\Delta E_{\mathrm{adh}} = \Delta E_{\mathrm{d}} - \Delta E_{\mathrm{a}}$). Thus, the fractional surface coverage is a function of the adhesive energy for any polymer-wall pair.

The physical basis of the unified model has been partially developed in our previous work [15], where we have discussed the solution of the TN model for constant ϕ (=1) leading to wall slip in the capillary flow due to disentanglement. It was assumed that the capillary could be divided into two regions; an interfacial annular region of thickness equal to approximately one radius of gyration at the wall consisting of the adsorbed molecules, and the remaining bulk region. It was further argued that the dynamics of entanglement and disentanglement of the adsorbed chains are different from that of the bulk chains. It has been shown [15] that the constitutive equation reduces to two governing equations for the network model, which have to be solved independently in the annular wall region and in the bulk region. These equations are

$$\tau_{rz} = \frac{G_0\gamma_{\mathrm{e}}f}{g} = (n_0kT)n\gamma_{\mathrm{e}}, \tag{11}$$

$$\frac{\partial v_z^*}{\partial \mathrm{r}} = \frac{g\gamma_{\mathrm{e}}}{We\,R}, \tag{12}$$

where superscript $*$ indicates non-dimensionalized variables ($v_z^* = v_z/v_m$), $We = \lambda v_m/R$ is the Weissenberg number, λ the relaxation time, R is the radius of the capillary, v_m is the maximum velocity, n ($=f/g$) are the number of entanglements per unit volume under flow normalized with respect to the equilibrium number of entanglements n_0, and f and g are the rates of creation and the loss of entanglements, respectively.

As long as the interfacial network is intact (i.e. before strong slip) the stress in the annular region is only due to the contribution from the segments of the adsorbed chains. Hence, Eq. (11) for the annular region can be written as

$$\tau_{rz} = \phi \frac{G_0 \gamma_e f}{g} = (\phi n_0 kT) n \gamma_e. \tag{13}$$

Eqs. (12) and (13) can be solved provided the rates of entanglement and disentanglement under flow are known. When f and g are related to the end-to-end distance of network segments $\left\langle \tilde{\boldsymbol{Q}} \cdot \tilde{\boldsymbol{Q}} \right\rangle$ [18], one does not typically obtain a closed form constitutive equation. Towards this objective, f and g can be empirically related to the effective strain [15,19,20]. The functions f and g used in the present analysis are those proposed by Ahn and Osaki [19,20].

$$f = \exp(a\gamma_e), \qquad g = \exp(b\gamma_e). \tag{14}$$

The above functions when used in Eq. (13) yield a non-monotonic stress–strain rate relationship for $b > a$. A maximum in stress occurs at $\gamma_e = 1/(b-a)$. We have shown that such non-monotonic behavior represents severe disentanglement ($g > f$) due to chain stretching [15]. At the stress maximum, the chains undergo a transition in the end-to-end distance, akin to the coil to stretch transition predicted by [3].

Now let us consider the interfacial annular wall region. Eq. (14) along with Eqs. (12) and (13) constitute a set of equations that need to be solved in the annular wall region. It can be seen from Eq. (13) that in the annular region the contribution to the wall-shear stress is from three interdependent variables: (i) ϕ, the fractional surface coverage, which depends on the dynamics of adsorption and desorption and decreases with increase in γ_e and temperature, (ii) γ_e, the effective strain, which represents the stretching of chains and (iii) f/g, which decreases with γ_e for severe disentanglement ($b > a$). Thus, Eq. (13) can predict a non-monotonic local stress–strain rate relationship by two independent mechanisms. For a low surface energy wall, $\phi\gamma_e$ will show a stress maximum due to desorption of macromolecules (a decrease in ϕ). For a high surface energy wall disentanglement of adsorbed chains will occur due to the chain stretching at constant fractional surface coverage ϕ and the stress maximum will occur due to $\gamma_e f/g$.

When strong slip occurs, either by a debonding or by a disentanglement mechanism, the network in the annular wall region is disrupted. Therefore, the TN model would cease to hold. Stress transfer occurs primarily by friction as the bulk slides over the bare wall in the case of debonding or over the carpet wall (the carpet being formed due to the stretched adsorbed chains on the wall) in the case of disentanglement. A 'friction law' can be written in a simple empirical form as proposed by de Gennes [21]

$$v_s = k'\tau_w, \tag{15}$$

where k' is the friction coefficient. The various forms of k' for bare wall and carpet wall with different surface coverages have been developed by Ajdari et al. [10] and Brochard-Wyart et al. [11]. In the current model k' has been taken to be a fitting parameter.

We solve Eqs. (11) and (12) in the bulk region, and Eqs. (12) and (13) in the annular wall region before the onset of a strong slip regime. The model parameters common to the bulk and annular regions are G_0 and λ. However, the model parameters related to the entanglement and the disentanglement (namely, *a* and *b* in Eq. (14)) are different in the bulk and wall regions. The physical picture behind this assumption is as follows. The bulk chains can relax by several mechanisms such as reptation, convective constraint release, fluctuations and chain stretching. However, a tethered chain cannot reptate as long as it is attached to the wall. Therefore, it is probably more susceptible to getting orientated and stretched. Hence, the inherent dynamics of tethered chains as represented by *a* and *b* in a network model is expected to be different than that of the bulk chains. The parameters related to kinetics of adsorption and desorption are *A* and ΔE_{adh}. *A* in Eq. (10) is treated to be curve a fitting parameter, while the adhesive energy ΔE_{adh} is taken from the available data in the literature. At the interface of both the regions, the continuity of the stress and velocity is maintained. After the stress maximum in the annular region, the interfacial region ceases to exist either due to loss of complete surface coverage or due to the stretched and fully disentangled chains. Therefore, after strong slip the slip boundary condition is considered (Eq. (15)) at the wall.

3. Results and discussion

3.1. General predictions

As discussed earlier, the non-monotonic stress–strain rate relationship at the wall results in a first order transition in the flow rate (i.e. strong slip). Fig. 2 shows a qualitative model prediction of wall shear stress versus slip velocity before and after a strong slip. The slip velocity before the first-order transition (weak slip) is the velocity of the bulk chains at the interface of the annular region. This is calculated from the network model. After strong slip, the slip velocity is calculated from Eq. (15). The transient network

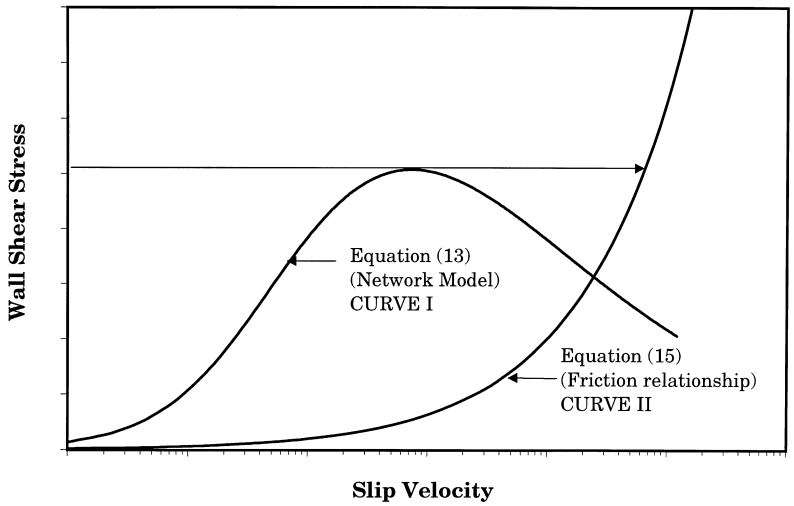

Fig. 2. A schematic of model prediction. Curve I shows the flow behavior before strong slip. In this region the slip velocity (interfacial) depends on the network dynamics. The non-monotonic behavior can arise either from disentanglement or debonding. After strong slip, stress transfer is due to the friction represented by curve II.

model, when solved in the annular wall region predicts a non-monotonic wall shear stress as shown by curve I in Fig. 2. The non-monotonic nature can arise due to disentanglement or due to debonding. Curve II in Fig. 2 represents either the monomer–monomer friction (in the case of disentanglement) or the monomer-wall friction (in the case of debonding). In a controlled stress experiment the slip velocity will jump from curve I to curve II at the stress maximum. Such a first order transition in the slip velocity will result in a first-order transition in the flow rate. If curve I merges with curve II without going through the maximum, then the model will predict a continuous slip without any first-order transition. This phenomenon has been observed in the case of some polymers such as LDPE. The exact nature of Curve I and II will depend on the dynamics in the polymer–wall interfacial region, which will be governed by the molecular structure of the polymer and the characteristics of the wall–polymer interaction.

Fig. 3a shows a qualitative prediction of the fractional surface coverage (ϕ) and the non-monotonic wall-shear stress with respect to slip velocity. It can be seen that the fractional surface coverage (ϕ) remains constant while the wall-shear stress goes through a maximum. The decrease in wall-shear stress at constant ϕ indicates that the slip occurs by disentanglement for the high value of adhesive energy indicated in Fig. 3a. If the adhesive energy is progressively decreased while keeping the other parameters constant, then the slip occurs by debonding. Fig. 3b shows wall-shear stress and ϕ as a function of the slip velocity at a lower value of the adhesive energy. Other parameters have been kept the same as in Fig. 3a. The surface coverage and wall-shear stress rapidly decreases at the same slip velocity confirming that the slip is due to debonding. Thus, the model is able to predict the wall slip by both disentanglement and debonding mechanisms and unifies them into one mathematical formalism. The critical model parameter, which governs the mechanism, is the adhesive energy.

An important prediction of the unified slip model is the temperature dependence of slip parameters namely, the slip length $b(T)$ and $\tau_c(T)$. The slip length is defined as [1]

$$b = \begin{cases} \dfrac{\eta_B}{\eta_I} a & \text{disentanglement,} \\ \eta_B k' & \text{debonding,} \end{cases} \tag{16}$$

where η_B is bulk viscosity, η_I the interfacial viscosity, a the monomer length scale and k' is the friction coefficient of ungrafted bare wall. Both interfacial and bulk viscosity are identically scaled with temperature (i.e. they decrease with increase in temperature). Thus, b would be independent of temperature in the case of disentanglement. Further, $k' = a_m^2/\zeta_m$, a_m being the monomer length and ζ_m is the monomeric friction coefficient, which decreases with increase in temperature [13]. Hence, k' increases with decrease in temperature. Thus, b would be independent of temperature in the case of debonding also. Hence, the temperature dependence of the slip length cannot be used to discuss the governing mechanism of slip.

We show that in fact the temperature dependence of the critical stress (not slip length) might be used to distinguish between the two slip mechanisms. The temperature dependence of stress arises from three factors: the temperature dependence of the network dynamics, the activation terms in the adsorption–desorption kinetics and the temperature dependence of the stress induced desorption kinetics. It can be seen from Eq. (10) that in the absence of flow, the fractional surface coverage (ϕ) decreases with increase in temperature. In the presence of flow, the surface coverage tends to decrease further with increase in temperature. On the other hand, the modulus of the network tends to increase with temperature and the relaxation time decreases with increase in temperature. All these different temperature dependent factors influence the critical wall-shear stress. The parameter A in Eq. (10) plays a crucial

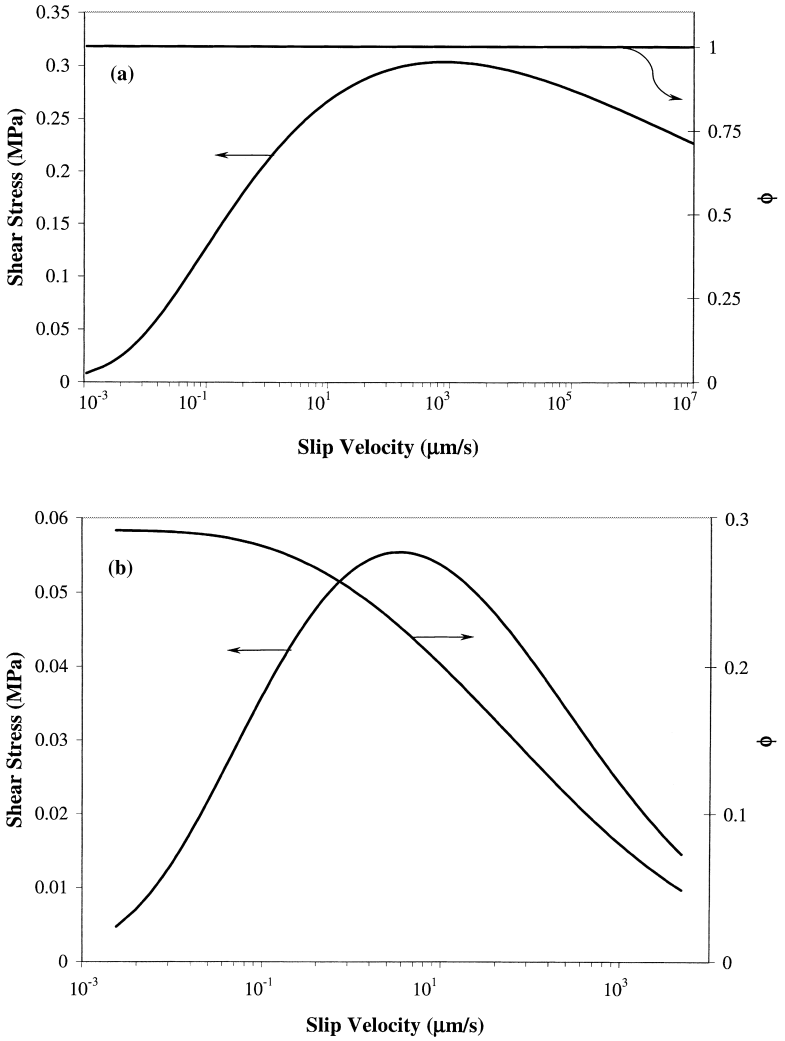

Fig. 3. A plot of fractional surface coverage and shear stress vs. slip velocity. The slip mechanism is dependent on the adhesive energy of the wall–polymer pair. The model parameters are $A = 0.0047$, $T = 473\,\mathrm{K}$, $n_0 = 1.265\mathrm{E}{+}26$ ($G_0 = 0.547\,\mathrm{MPa}$ at 200°C). In the interfacial region $a = 8.0$, $b = 9.0$. (a) At high surface energy ($\Delta E_{\mathrm{adh}} = 2.827\mathrm{E}{-}19\,\mathrm{J}$ per molecule) the non-monotonic behavior is due to disentanglement. The surface coverage remains constant; (b) if adhesive energy is decreased ($\Delta E_{\mathrm{adh}} = 2.921\mathrm{E}{-}20\,\mathrm{J}$ per molecule) keeping all other parameters constant, slip occurs due to debonding and stress and surface coverage drop simultaneously.

role in determining the temperature dependence of critical wall-shear stress. The parameter A considers the concentration of unattached polymer chains in the vicinity of the bare wall. The value of parameter A can in principle be calculated from the equilibrium surface coverage data. A controls the equilibrium fractional surface coverage (ϕ_{eq}) such that ϕ_{eq} increases with increase in A. However, in the absence of any data on adsorption of chains from melts, we are forced to consider A as a curve fitting parameter in our model.

Fig. 4a–c show critical wall-shear stress vs. desorption energy at two different temperatures and for various values of A. In general, three regions of temperature dependence can be seen in these figures. The first region corresponds to disentanglement, while the last two regions correspond to debonding. It can be seen that at high values of adhesive energies the critical stress is independent of the adhesive energy irrespective of the value of A. The governing mechanism in this region is disentanglement and the critical stress is also seen to be increasing with temperature as predicted by Brochard and de Gennes [3] and Joshi et al. [15]. The mechanism changes from disentanglement to debonding as the adhesive energy is progressively decreased. In the third region, where slip occurs by debonding, the temperature dependence is surprisingly similar to that in the first region. The critical wall-shear stress increases with temperature and this dependence is independent of the value of A. For very low values of the adhesive energy, a small amount of stretching is sufficient to cause debonding. However, the extent of stretching decreases with temperature and therefore, higher stress is required for debonding to occur. Hence, the critical shear stress increases with temperature. We wish to caution that in the third region the equilibrium fractional surface coverage is so low that the transient network model may not be really applicable.

The effect of parameter A is seen in the second region of Fig. 4a–c. In Fig. 4a it can be seen that as the mechanism changes from disentanglement to debonding in the second region, the temperature dependence of the critical stress also reverses. For these values of A, i.e. for high ϕ_{eq}, the critical stress decreases with an increase in temperature. Such inverse temperature dependence was intuitively suggested by Wang and Drda [9]. Our model is the first to predict it mathematically. Thus, the temperature dependence of the critical stress could be an indicator of the governing slip mechanism. However, the parameter A determines the temperature dependence. For high values of A, i.e. for high ϕ_{eq}, the critical stress increases with an increase in temperature over the full range of adhesive energies as seen in Fig. 4c. Only for low values of A and for the intermediate values of adhesive energies, the temperature dependence of critical wall-shear stress is different for disentanglement and debonding mechanisms (see Fig. 4b). We will show in the subsequent work [22] that experimental determination of the temperature dependence of critical stress on a fluoropolymer coated surface (of low adhesive energy) validates the inverse temperature dependence.

We have shown that our model successfully unifies the two mechanisms into one mathematical framework. It predicts that the adhesive energy between the polymer wall pair is the governing parameter determining the operative mechanism. It also predicts the temperature dependence of critical wall-shear stress. However, our model suffers from certain drawbacks owing to its inherent simplicity. For instance the prediction of the stress–slip velocity curve by the network model when $b > a$, does not show a minimum in stress. The stress decreases continuously in a manner predicted in the original Doi–Edwards model. The absence of a stress minimum in the Doi–Edwards model is due to the absence of chain stretching [23]. The friction law takes care of the stress transfer to the tethered chains or on the bare wall in the strong slip region, which shows an increase in stress with slip velocity. In the present model, since our major concern is identifying the stress at which the instability begins and not to develop a slip law in the strong slip region, we have made use of the friction law.

3.2. Comparison with experimental results

We will now compare our model predictions quantitatively with some of the available experimental data on slip in polymer melts. The details regarding the model parameters have been already discussed in the previous section. To compare the experimental results with the model predictions the adhesive energy values reported in literature are used. Hill [4] has reported the adhesive energy of the polyethylene–steel

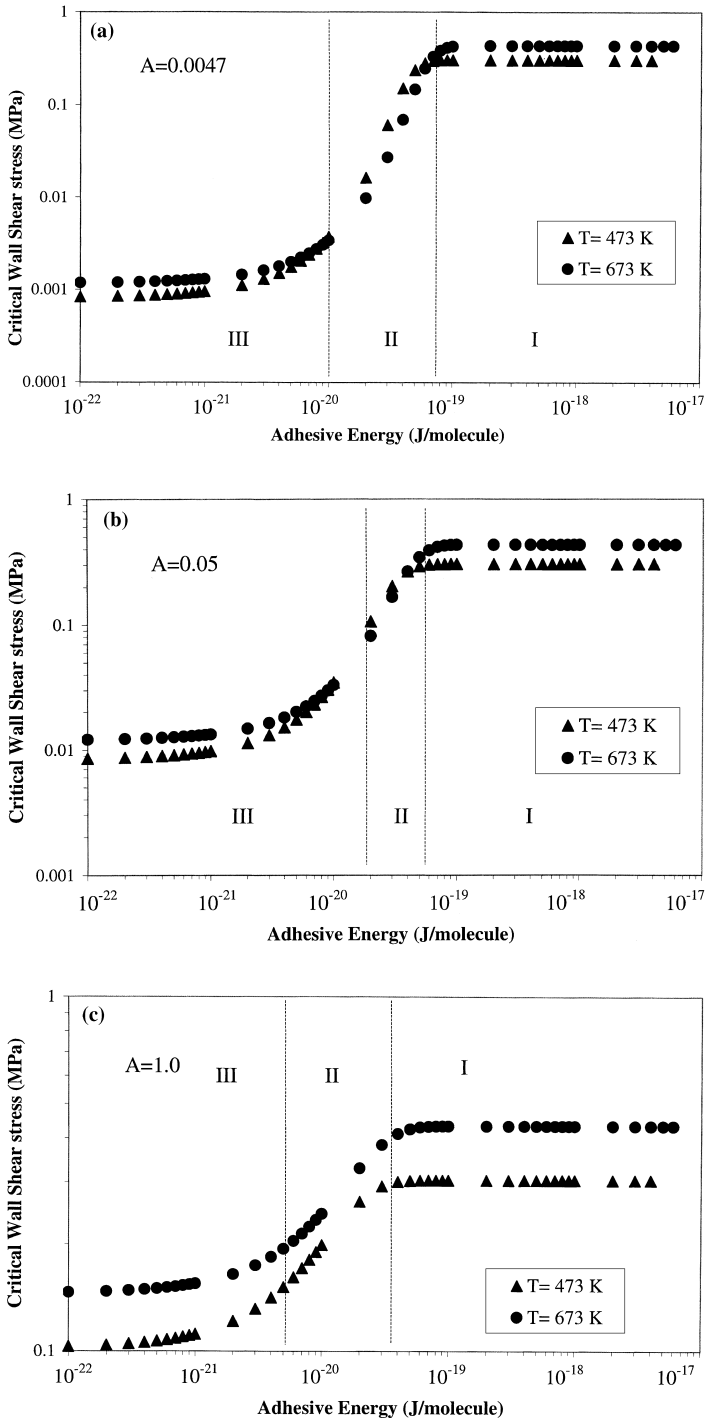

Fig. 4. The temperature dependence of critical stress over the range of adhesive energies is shown. In the first and third regions, the temperature dependence is independent of A, while in the second region with increase in A the temperature dependence reverses. The first region corresponds to disentanglement, while the other two regions correspond to debonding. The model parameters are the same as in Fig. 3.

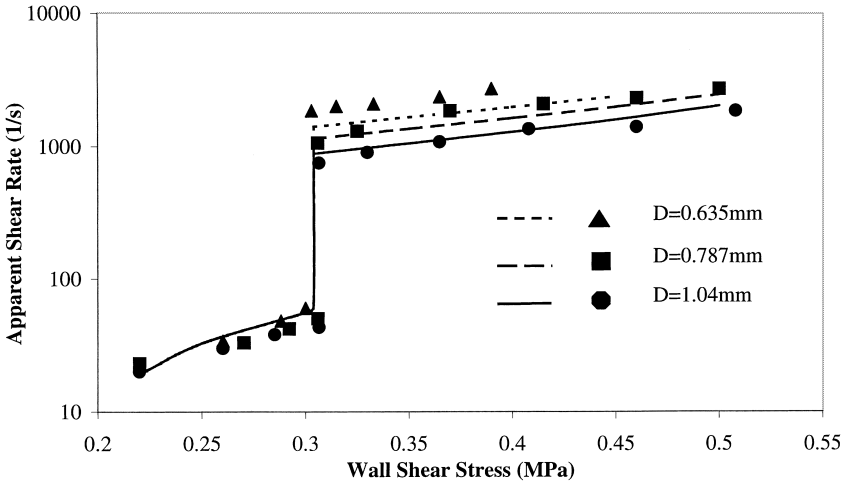

Fig. 5. A Comparison of the model prediction for apparent shear rate vs. wall shear stress with polyethylene melt experimental data [14]. The flow curve for $D = 1.04$ mm is fitted using model parameters same as that in Fig. 3a with $\lambda = 0.1$ s, in bulk, region $a = 8.0$, $b = 8.0$ and $k' = 7\text{E}{-7}$. Flow curves for other diameters are predictions. Points represent the experimental data and the line represents the model fit.

pair (difference between polymer–metal work of adhesion and polymer–polymer work of cohesion) to be 90 mJ/m^2. This adhesive energy is converted into (energy)/(adsorption junction) or (energy)/(adsorbed molecule) by using the equilibrium surface coverage density based on the assumption that only a single junction on the wall is present in the circular area of 1 nm radius. Fig. 5 shows a quantitative fit of our model to the slip data for high-density polyethylene [14]. For this high value of adhesive energy the model

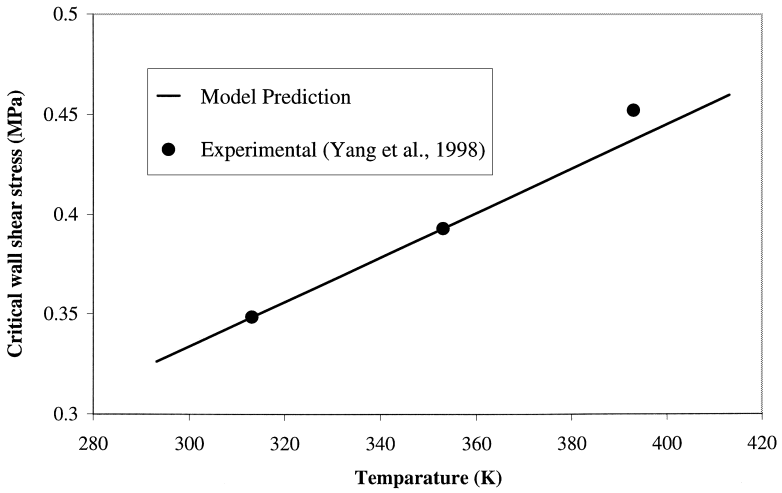

Fig. 6. A comparison of the model prediction for critical wall shear stress vs. temperature experimental data [8]. The model parameters are, $A = 0.0047$, $T = 313$ K, $\Delta E_{\text{adh}} = 2.827\text{E}{-19}$ J per molecule, $n_0 = 2.314\text{E}{+26}$ ($G_0 = 1$ MPa at 40°C). In the interfacial region $a = 8.0$, $b = 9.056$.

Table 1
The adhesive energy and critical wall shear stress data for various wall–polymer pairs from Anastasiadis and Hatzikiriakos [24]

Polymer–wall system	The adhesive energy given in (energy/area) (dyn/cm)	Converted form of adhesive energy in (energy/molecule) (J per molecule)	Corresponding critical wall shear stress (MPa)
LLDPE–steel	22.6	7.098E−20	0.1
LLDPE–Teflon®	9.3	2.921E−20	0.027

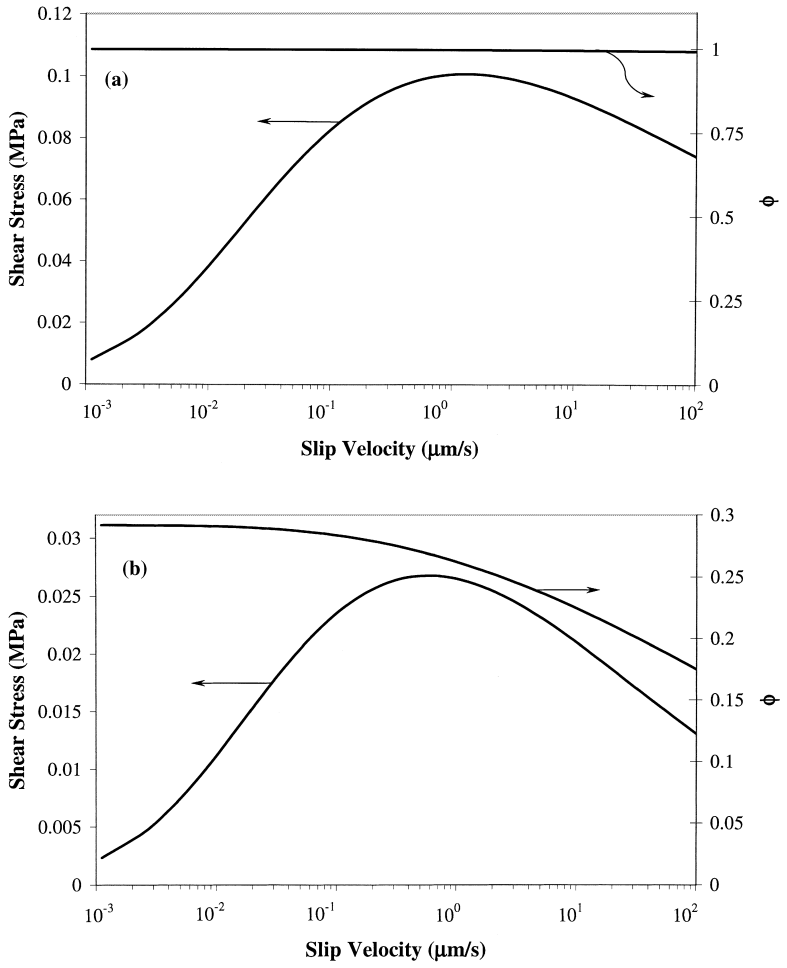

Fig. 7. Comparison of adhesive energy and critical wall shear stress [24]. The model parameters are $A = 0.0047$, $T = 473$ K, $n_0 = 1.265\text{E}{+}26$ ($G_0 = 0.547$ MPa at 200°C). In the interfacial region $a = 8.0$, $b = 11.0$. (a) For adhesive energy corresponding to LLDPE-steel ($\Delta E_{\text{adh}} = 7.098\text{E}{-}20$ J per molecule). The slip is considered to be by disentanglement; (b) for adhesive energy corresponding to LLDPE-Teflon® ($\Delta E_{\text{adh}} = 2.921\text{E}{-}20$ J per molecule) the model correctly predicts critical stress by debonding.

predicts slip to occur by a disentanglement mechanism. The network modulus G_0 is approximately of the order of the plateau modulus (for polyethylene, the plateau modulus is ∼2.6 MPa). The model successfully predicts the first order transition in flow rate along with the diameter dependent flow curves. The diameter dependence originates from the difference between the network dynamics in the bulk and interfacial region and can also be predicted in the case of a debonding mechanism by our model.

The model also successfully predicts the temperature dependence of critical wall-shear stress. Fig. 6 shows the critical wall-shear stress plotted against temperature. The points show the experimental data for polybutadiene on a steel surface [8]. It can be seen that the model fits the experimental data quantitatively, when the disentanglement is assumed to be the governing mechanism. In this case the network modulus G_0 has been assumed to be the same as the plateau modulus of the polymer ($G_0 = 1.0$ MPa, or $n_0 =$ 2.314E+26 at 200°C).

Recently Anastasiadis and Hatzikiriakos [24] have measured the adhesive energies of various polymer–metal pairs using the pendent drop method. They have also compared the critical wall shear stress data with the adhesive energy. We feel that the fit of such data will give a better test of the model. We have considered the experimental data of LLDPE on steel as well as on Teflon® in this work. The adhesive energy given in (energy)/(area) has been converted to (energy)/(adsorbed molecule) as discussed earlier (See Table 1). Here we presume that the system of LLDPE on steel shows slip due to disentanglement. The model successfully fits the critical stress as shown in Fig. 7a. The constant fractional surface coverage confirms slip by disentanglement. Keeping all the other parameters constant, if the adhesive energy is changed to that for LLDPE on Teflon®, the model not only successfully predicts slip due to debonding but also predicts the experimentally observed critical wall-shear stress for the same system (see Fig. 7b).

As it stands, the model has two curve fitting parameters. The network parameters for the chain dynamics in the interfacial region ($a - b$) can be obtained from independent experimental data on confined melts. The parameter A can be obtained from equilibrium surface coverage data. G_0 is obtained from the plateau modulus while the bulk parameters such as a, b and λ are to be fitted to viscometric data. If this is done, then no curve fitting parameters will be required and the model will become fully predictive.

4. Conclusion

A unified slip model is developed, which shows slip by either mechanism (disentanglement or debonding) depending on the adhesive energy. It is shown that in the case when either of the mechanisms prevail, the local non-monotonic stress-shear rate behavior near the wall of the adsorbed molecules is necessary to show the first-order transition in flow rate. The non-monotonic behavior near the wall (the annular wall region) arises through a coil to stretch transition for a high surface energy wall (disentanglement), while it arises through the desorption of the adsorbed molecules for a low energy wall. After a strong slip (in both the cases), the stress transfer is assumed to arise from friction between the bulk molecules with either the carpet wall (disentanglement) or the bare wall (debonding).

The model predicts the diameter dependence of the flow curves for both disentanglement and debonding mechanisms. We believe that the diameter dependence arises from different flow behaviors (network dynamics) in the bulk and near the wall. For the case of disentanglement the model shows a direct dependence of the critical wall-shear stress on temperature, while for debonding, this dependence is determined by the equilibrium surface coverage.

References

[1] S-Q. Wang, Molecular transitions and dynamics at polymer/wall interfaces: origins of flow instabilities and wall slip, Adv. Polym. Sci. 138 (1999) 227–275.
[2] L. Léger, E. Raphaël, H. Hervet, Surface-anchored polymer chains: their role in adhesion and friction, Adv. Polym. Sci. 138 (1999) 185–225.
[3] F. Brochard, P.G. de Gennes, Shear-dependent slippage at a polymer/solid interface, Langmuir 8 (1992) 3033–3037.
[4] D.A. Hill, Wall slip in polymer melts: a pseudo-chemical model, J. Rheol. 42 (1998) 581–601.
[5] D.S. Malkus, J.A. Nohel, B.J. Plohr, Dynamics of shear flow of a non-Newtonian fluid, J. Comp. Phys. 87 (1990) 464–487.
[6] T.C.B. Mcleish, R.C. Ball, A molecular approach to the spurt effect in polymer melt flow, J. Polym. Sci. Polym. Phys. Ed. 24 (1986) 1735–1745.
[7] Y.H. Lin, Explanation for slip–stick melt fracture in terms of molecular dynamics in polymer melts, J. Rheol. 29 (1985) 605–637.
[8] X. Yang, S-Q. Wang, A. Halasa, H. Ishida, Fast flow behavior of highly entangled monodisperse polymers. 1. Interfacial stick slip transition of polybytadiene melts, Rheol. Acta 37 (1998) 415–423.
[9] S.-Q. Wang, P.A. Drda, Molecular instabilities in capillary flow of polymer melts: interfacial stick–slip transition, wall slip and extrudate distortion, Macromol. Chem. Phys. 198 (1997) 673–701.
[10] A.F. Ajdari, F. Brochard-Wyart, P.G. de Gennes, L. Leibler, J.L. Viovy, M. Rubenstein, Slippage of an entangled polymer melt on a grafted surface, Physica A 204 (1994) 17–39.
[11] F. Brochard-Wyart, C. Gay, P.G. de Gennes, Slippage of polymer melts on grafted surfaces, Macromolecules 29 (1996) 377–382.
[12] S.G. Hatzikiriakos, N. Kalogerakis, A dynamic slip model for molten polymers based on a network kinetic theory, Rheol. Acta 33 (1994) 38–47.
[13] A.L. Yarin, M.D. Graham, A model for slip at polymer/solid interface, J. Rheol. 42 (1998) 1419–1504.
[14] S.Q. Wang, P.A. Drda, Super fluid like stick–slip transition in capillary flow of linear polyethylene melt. 1. General Features, Macromolecule 29 (1996) 2627–2632.
[15] Y.M. Joshi, A.K. Lele, R.A. Mashelkar, Slipping fluids: a unified transient network model, J. Non-Newtonian Fluid Mech. 89 (2000) 303–335.
[16] R.G. Larson, Constitutive equations for polymer melts and solutions, Butterworths Series in Chemical Engineering, Boston, 1988, pp. 34.
[17] W. Philippoff, On normal stresses, flow curves, flow birefringence, and normal stresses of polyisobutylene solutions. Part I. Fundamental principles, Trans. Soc. Rheol. 1 (1956) 95–107.
[18] F. Petruccione, P. Biller, A numerical stochastic approach to network theories of polymeric fluids, J. Chem. Phys. 89 (1988) 577–582.
[19] K.H. Ahn, K. Osaki, A network model predicting the shear thickening behavior of poly(vinyl alcohol)/sodium borate aqueous solution, J. Non-Newtonian Fluid Mech. 55 (1994) 215–227.
[20] K.H. Ahn, K. Osaki, Mechanism of shear thickening investigated by a network model, J. Non-Newtonian Fluid Mech. 56 (1995) 267–288.
[21] P.G. de Gennes, Wetting: statics and dynamics, Rev. Mod. Phys. 57 (1985) 827–863.
[22] Y.M. Joshi, P.S. Tapadia, A.K. Lele, R.A. Mashelkar, Temperature dependence of critical stress for wall slip by debonding, J. Non-Newtonian Fluid Mech., in press.
[23] M. Doi, S.F. Edwards, The Theory of Polymer Dynamics, Oxford University Press, London, 1986.
[24] S.H. Anastasiadis, S.G. Hatzikiriakos, The work of adhesion of polymer/wall interfaces and its association with the onset of wall slip, J. Rheol. 42 (1998) 795–812.